Reinforced soil wall measurements and predictions

Ehrlich, M.
Federal University of Rio de Janeiro, Rio de Janeiro, Brazil.

Becker, L.D.B.
Federal University of Rio de Janeiro, Rio de Janeiro, Brazil.

Keywords: reinforced soil, design methods, physical models, numerical analysis, case studies and soil compaction.

ABSTRACT: Analytical models for the analysis of reinforced soil structures are presented and discussed. The results of field studies, and numerical and laboratory physical modeling are also presented. Limit equilibrium methods are usually used to determine reinforcement tension. Although these models are very simple to understand they do not take into consideration important factors, e.g., soil and reinforcement deformability and the induced stress due to soil compaction. Working stress design methods have been developed to overcome these difficulties. Comparisons were made of measured and calculated values, and the prediction capability of available procedures was verified. Cases studies clearly illustrated that fine-grained tropical soils are excellent backfill material for reinforced soil wall construction, in spite of the usually high percentage of fines in such soils. Measurements in a reinforced embankment showed the effect of confinement on the stiffness of nonwoven geotextile and in the structure movements. The effect of wall facing and soil compaction on the behavior of the reinforced structures was also verified through case studies and physical and numerical modeling.

1 INTRODUCTION

Analytical models for determining the tension of reinforced soil structures are presented and discussed herein. The results of field studies, and numerical and laboratory physical modeling are also presented. Comparisons are made of measured and calculated values, and the prediction capability of some analytical procedures is verified. The use of fine-grained tropical soils as backfill in reinforced soil wall structures is supported by available case studies. The effect of wall facing and soil compaction on the behavior of reinforced soil structures is also indicated.

2 ANALYTICAL MODELS

Reinforced soil structures must be internally and externally stable i.e. they should not fail. Failure can be viewed as a performance problem, related to either strength or deformation.

It is widely accepted that the external stability analysis of reinforced soil structures should be carried out in the same way as stability analysis of traditional earth-retaining structures: the engineer has to be sure that the entire structure will not slide outwards, overturn or fail in bearing capacity.

The internal stability, however, is a more complicated subject. It is generally accepted that at least three conditions should be avoided: tension failure of the reinforcement, pullout failure and failure in the reinforcement/facing connection, but there are many different analytical models. The results of these models can be very different, even leading to unsafe designs in some situations.

This article will focus on analytical models for the prediction of maximum tension load in the reinforcements.

The prediction of the maximum tension force in every level of reinforcement (T_{max}) is one of the most important design steps in a reinforced soil structure. It was and, in many cases, is still done by limit equilibrium considerations. T_{max} is calculated by considering the forces required for local equilibrium i.e. the tension strength of the reinforcements and the shear strength of the soil (Steward et al. 1977; Leshchinsky and Boedeker 1989). Although these models are very simple to understand and use, they have important drawbacks: they simply disregard the effects of reinforcement deformability, soil

deformability, compaction and, in some cases, cohesion (Ehrlich and Dantas 2000).

Empirical and working stress design methods were developed to overcome these difficulties (Ehrlich and Mitchell 1994; Bathurst et al. 2003). These methods are based either on field monitoring of many structures or on more realistic approaches to the complex behavior of reinforced soil structures.

2.1 *Limit equilibrium models for design*

The models based on limit equilibrium are based on five assumptions: the structure is on the verge of collapse, the geometry of the failure surface is known, the soil behavior is rigid-perfectly plastic, the position of the reinforcements is known and there is full mobilization of shear resistance on the failure surface.

Unfortunately the assumptions of limit equilibrium models are far from reality. Well-designed structures are supposed to be far from collapse, the soil behavior is non-linear elasto-plastic, the location of the failure surface (if there is any) is not clearly known and, obviously, the shear resistance is not fully mobilized.

Some models assume a horizontal stress distribution that is counterbalanced by the tension forces in the reinforcements.

Instead of using only force equilibrium, other models assume circular or log-spiral failure surfaces and consider the reinforcement tension forces in slope stability calculations (force and moment equilibrium).

The method presented by Steward et al. (1977) is an early example of a method based on a limit equilibrium model intended for the design of geosynthetic reinforced walls.

The method is based on the assumption that a planar potential failure surface passes through the reinforcements and the toe of the structure sloping $45+\phi'/2$ from the horizontal. The reinforced soil block is divided into two zones: resisting and active.

The horizontal stress distribution is assumed to be linear:

$$\sigma'_x = K \cdot \gamma \cdot z$$

where K = earth pressure coefficient,
γ = unit weight of soil and
z = depth (in the absence of surcharges).

The next step is to set a vertical spacing for the reinforcements. The T_{max} in any reinforcement is the product of the average horizontal stress at that level, vertical spacing and some safety factor.

The engineer must check that the reinforcement length extending inside the resisting zone is sufficient to prevent pullout failure.

Steward et al. (1977) recommended the use of the earth pressure coefficient at rest. In an attempt to consider the deformability of the reinforced soils others prefer using the active earth pressure coefficient.

Leshchinsky and Boedeker (1989) proposed a model based on a log-spiral failure surface that can be used for inclined facings. The maximum tension force is found at the lowest reinforcement level:

$$T_{max}^{lowest} = T_m \cdot FS \cdot \gamma \cdot H^2 / n$$

where FS = factor of safety,
H = structure height and
n = number of reinforcement levels.

T_m can be obtained from the graph shown in Figure 1. The tangent of the angle formed by the horizontal and the facing is "m". A vertical facing is therefore represented by $m = \infty$.

It should be noted that, for vertical slopes, $T_m = K_a$ and that this method is similar to the previous one.

However, the basic models of limit equilibrium based methods are inaccurate because of the disregard for compaction and both soil and reinforcement strains.

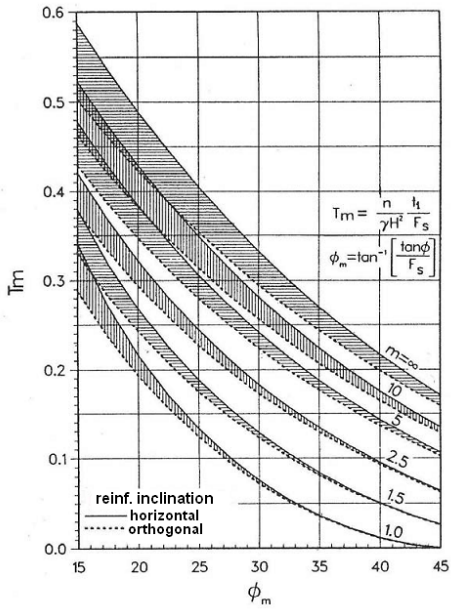

Figure 1. Curves for calculation of T_{max} (Leshchinsky and Boedeker 1989).

2.2 *Empirical models*

Empirical models may be developed based on statistical treatment of data from monitoring of actual structures. Although these models can implicitly consider many factors affecting the reinforced soil behavior their accuracy depends on the number of monitored structures and data reliability.

Their predictions are usually valid for structures with similar features like soil type, compaction equipment and reinforcement strength/deformability.

Bathurst et al. (2003) presented a design method based on monitoring 30 geosynthetic reinforced soil structures built with granular backfills.

The maximum tension force at any level of geosynthetic reinforcement is:

$$T_{max} = ½ \cdot K_o \cdot \gamma \cdot (H+S) \cdot S^i_v \cdot D_{tmax} \cdot \Phi_{g,\,l,\,fs,\,fb}$$

where K_o = earth-pressure coefficient at rest for plane strain condition,
S = equivalent surcharge height,
S^i_v = vertical spacing at any level,
D_{tmax} = empirical coefficient for stress distribution according to foundation conditions and reinforcement type and position and
$\Phi_{g,\,l,\,fs,\,fb}$ = empirical coefficients for spacing, reinforcement deformability, facing type and facing inclination.

2.3 *Strain compatibility models for design*

Working stress design methods were developed to overcome the inaccuracy of limit equilibrium models (Adib 1988; Abramento and Whittle 1993; Ehrlich and Mitchell 1994; Dantas and Ehrlich 2000).

These models are based on strain compatibility assumptions – a more realistic approach to the complex behavior of reinforced soil structures. Sophisticated constitutive models for the stress-strain behavior of soil and reinforcement are needed.

Ehrlich and Mitchell (1994) proposed a model based on the strain compatibility between soil and reinforcement that accounts for soil and reinforcement stress-strain behavior and soil compaction. The reinforcement is considered as a linear elastic material. The soil is represented by a hyperbolic stress strain model modified from the one proposed by Duncan et al. (1980).

The compaction process model proposed by Duncan and Seed (1986) was simplified to a single cycle of load and unload. After the removal of the compaction equipment the vertical stress is reduced to its gravitational value, but horizontal residual stresses remain in the soil. For wall heights up to 6 m, the residual stresses induced by compaction may be much higher than the horizontal stress due to self weight, thereby causing a remarkable increase in maximum tension forces in the reinforcement.

Figure 2 shows the stress path assumed in the model. Point (1) represents the state of stress after placing a layer of soil, (2) during operation of the compaction equipment, (3) after compaction and (4) after the placing of another soil layer. The operation of the compaction equipment increases the vertical effective stresses to $\sigma'_{zc,i}$, where $\sigma'_{zc,i}$ is the maximum vertical stress induced due to compaction.

The horizontal effective stress is also increased to a maximum. At the end of the compaction equipment operation the vertical effective stress is reduced back to its initial value. However, the horizontal stress reduction is much smaller because the soil is not an elastic material. The placement of another layer will increase the vertical stress but the horizontal stress will remain almost the same. The effect of compaction will vanish only when the vertical stress induced by self weight surpasses the one induced by compaction. The height of soil (Z_c) necessary to achieve this depends on the compaction equipment and soil type. For typical compaction conditions a soil height of 6 m could be considered as a first approximation. The compaction equivalent influence depth Z_c can be calculated as follows:

$$Z_c = \sigma'_{zc,i} / \gamma$$

If there were no compaction at all, (1), (2) and (3) would lie on the same point. Both the horizontal effective stress and tension force in the reinforcement would be lower.

Ehrlich and Becker (2009) presented a chart for estimating the vertical effective stresses induced by some roller compactors in a soil of 18 kN/m³ unit weight and various friction angles. This is shown in Figure 3.

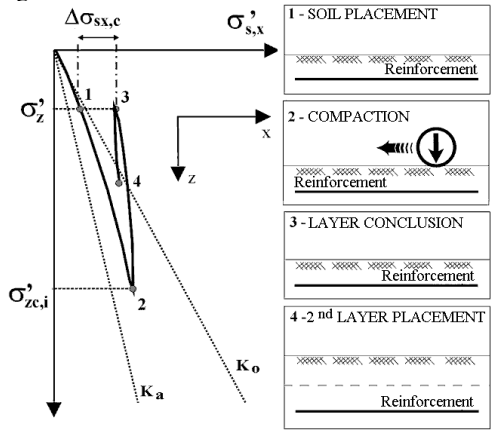

Figure 2. Effective stress path of a point inside the soil mass during the construction and compaction of an earth fill.

Due to the complexity of the model it would require cumbersome calculations to determine T_{max}. However the authors provided a series of charts to ease the user's task. New charts were further developed to account for cohesion and non vertical facings (Dantas and Ehrlich 1999). For example, Figure 4 presents charts for vertical walls built with cohesionless soils. The use of the charts requires knowledge of various parameters:

$$\beta = (\sigma'_{zc} / P_a)^n / S_i$$

$S_i = J / (K \cdot P_a \cdot S_v)$

where β = reinforcement deformability parameter for any level of reinforcement,
σ'_{zc} = maximum vertical stress at the considered level (geostatic or induced by compaction, whichever is greater),
P_a = atmospheric pressure,
n = modulus exponent of the hyperbolic model (Duncan et al. 1980),
J = tension modulus of reinforcement,
K = initial tangent modulus of the hyperbolic model (Duncan et al. 1980) and
S_v = vertical spacing.

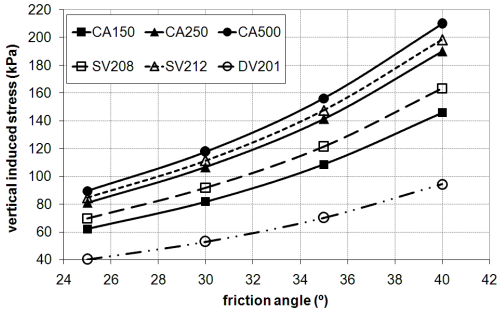

Figure 3. Vertical stresses induced by roller compactors.

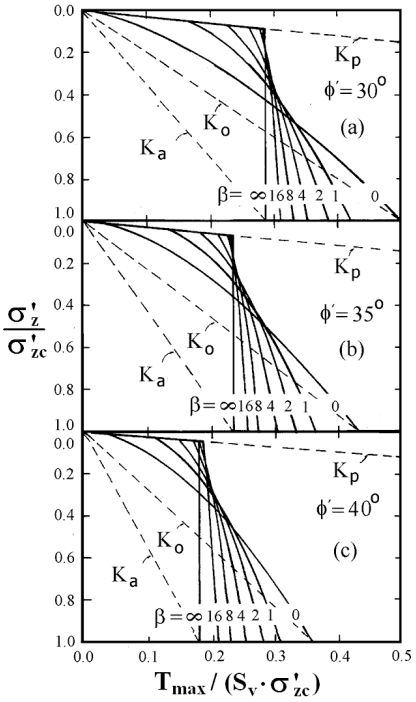

Figure 4. Charts for calculation of T_{max} for vertical walls built with cohesionless soils (Ehrlich and Mitchell 1994).

3 FIELD STUDIES

3.1 *Introduction*

Fine-grained residual soils have been widely used for many decades as backfill for reinforced soil wall and embankment construction in Brazil. Good performance of those structures has been verified (Carvalho et al. 1986; Ehrlich et al. 1994; Bruno and Ehrlich 1997; Ehrlich et al. 1997; Ehrlich, 1999; Bueno et al. 2006; Becker, 2006; Riccio and Ehrlich, 2009). Mori et al. (1979) discuss the properties of some typical compacted Brazilian saprolites. Tropical soils such as saprolites and lateritic soils, no matter what their percentage of fines, generally show good compaction and workability characteristics. The compacted soil has high strength, low compressibility and low permeability, even when compacted with water content above or below the Proctor optimum water content.

Those soils usually show significant apparent cohesion due to suction and also some true cohesion also.

Data from two of these monitored structures are shown below.

3.2 *SP123 Highway Embankment*

A 10-meter high geotextile reinforced soil embankment, with a backfill slope of 1H:2V, was built as part of an embankment to rebuild a section of highway SP-123 in São Paulo, as described by Carvalho et al. (1986) and Ehrlich et al. (1997). A landslide had previously occurred in this section.

Figure 5 shows the embankment section. The middle section, called Embankment II, was reinforced. The length and the vertical spacing of reinforcement was 7 m and 0.6 m, respectively.

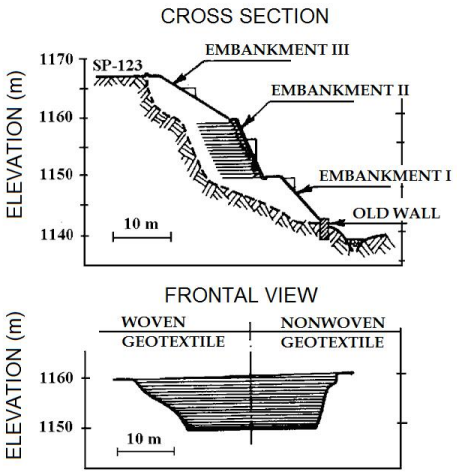

Figure 5. Embankment cross section and frontal view of SP123 Highway (Carvalho et al. 1986).

Two different types of reinforcement with the same unconfined tensile strength were used in the slope construction, in order to compare the effect of reinforcement type on embankment behavior: a nonwoven polyester geotextile was used on one half and a woven polypropylene geotextile on the other. The backfill material consisted of a compacted fine-grained tropical soil. Blocks of concrete were used for the facing.

The unconfined tensile strength of both geotextiles was 22 kN/m and elongation at failure was 10% and 39% for the woven (ASTM d-162) and nonwoven (AFNOR G38014) geotextile, respectively.

Table 1 presents the grain-size distribution and Atterberg limits for these soils. Also included in Table 1 are the shear resistance parameters for representative field moisture content and dry unit weight, i.e. 18% and 15.3 kN/m^3, respectively, where w_L is the Atterberg's liquid limit and PI is the plasticity index.

Table 1. Soil characteristics and shear resistance parameters

≤ 2μm (%)	≤ 20μm (%)	≤ 2mm (%)	w_L (%)	PI (%)	cohesion (kPa)	friction angle (°)
5	26	94	44	14	22	35

Global stability analysis using Bishop's (1955) modified method of analysis together with the parameters from laboratory tests led a safety factor of 1.48.

Figure 6 shows the horizontal and vertical movements measured at different points in Embankment II, just before and after the construction of Embankment III. Movement measurements were made using telltales and settlement plates. Dashed and solid lines represent measurements in the nonwoven geotextile and woven geotextile sections respectively.

Figure 6 shows that the nonwoven polyester geotextile section exhibited the lowest movement. This general trend persisted except at the top of the slope where the geotextile confinement was lower. At the top of the slope the horizontal movements were almost the same for the two sections. The stiffness of the nonwoven geotextile is greatly influenced by confinement (Jewell 1980; Andrawes et al. 1984). The effects of confinement on the nonwoven geotextile are shown in the analysis of the movements that occurred in Embankment II due to construction of Embankment III. The increase in horizontal movement in the nonwoven geotextile section was lower at the bottom than at the top of the slope, where there was less confinement. The movement increments decreased almost linearly with depth.

The performance of this embankment has been very good. All measurements show that the slope was stable during and after construction, including during period of rainfall. The ratio of measured horizontal movements and reinforced slope height was lower than 1.2%.

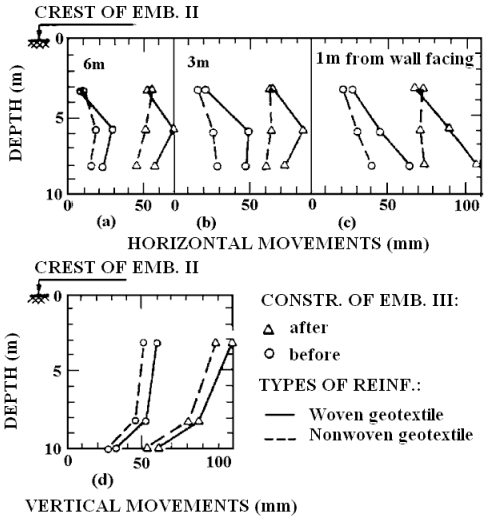

Figure 6. Horizontal and vertical movements measured in Embankment II (Ehrlich et al. 1997).

3.3 *São José dos Campos RSW*

An instrumented block-faced geogrid wall was built and monitored in São José dos Campos, SP, Brazil (Riccio and Ehrlich 2009; Riccio and Ehrlich 2010). Fine-grained tropical soils were used as backfill for the wall construction. The wall height in the instrumented section was 4.2 m. Monitoring was carried out for two months, including the construction phase.

The wall facing is composed of segmental precast concrete blocks (TERRAE W type block) with geogrids being used as reinforcement (FORTRAC models 55/30-20 and 35/20-20). A deep soft clay deposit is found in the area. The wall was constructed on a piled concrete platform. Two soil types were used as backfill: a yellow sandy clay (soil A), used from the top of the wall to 3.2 m depth, and a red sandy clay (soil B), used from 3.2 m to the bottom of the wall at 4.2 m depth. Table 2 shows the grain-size distribution and Atterberg limits for these soils. A Dynapac CA 250 PD roller was used for soil compaction.

Table 2. Soil characteristics in the S. José dos Campos RSW

Soil	≤ 2 μm (%)	≤ 20 μm (%)	≤ 2 mm (%)	w_L (%)	PI (%)
A	42	49	99	38	22
B	42	47	99	49	29

Table 3 shows the results of triaxial and plane-strain tests (CW – constant water content). The soil samples were compacted statically with a representative

field moisture content and density. Tests were performed with constant water content and controlled air pressure inside the soil sample (atmospheric pressure). The pore-water pressure was measured during these tests, where w is the water content, ϕ'is the effective friction angle and c_{eq} is the equivalent soil cohesion that includes the effect of pore-water suction on shear resistance.

Table 3. Laboratory test results (Riccio and Ehrlich 2009)

Soil	Test type	γ (kN/m^3)	w (%)	ϕ' (°)	c_{eq} (kPa)
A	Plane Strain	16.7	20	36	60
	Triaxial	16.5	21	25	42
B	Plane Strain	16.7	20	38	50
	Triaxial	16.5	21	26	52

Five different reinforcement layers were monitored at four different points using load cells along its length. Figure 7 shows the tension distributions measured in the reinforcements at the end of the construction phase. The 0 cm position represents the facing.

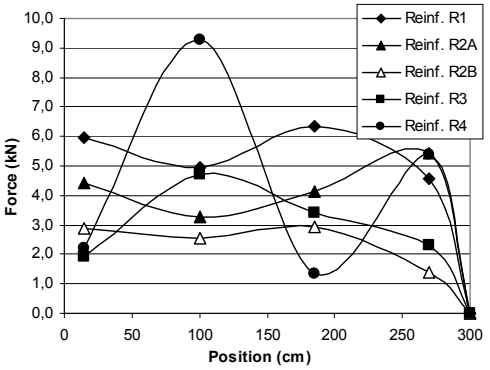

Figure 7. Reinforcement tension at the end of construction (Riccio and Ehrlich 2009).

Figure 8 shows the relationship between the maximum reinforcement tension and depth. Note that there is no tendency for an increase with depth, in accordance with the model of Ehrlich and Mitchell (1994). This behavior was due to high induced horizontal stress due to compaction and low stiffness reinforcements.

Figure 9 shows the tension measurements in a monitored reinforcement layer before, during and after the operation of the compaction equipment. An increase in peak stress may be seen in the reinforcement tension induced by the operation of equipment, followed by an unloading to a residual tension value at the end. The residual value is much higher than the value found before soil compaction. The observed behavior is also consistent with Ehrlich and Mitchell's (1994) model. It is interesting to note that the residual stress is not uniform along the length of the reinforcement. The final value for load cell set 3 was higher than that for the other load cells.

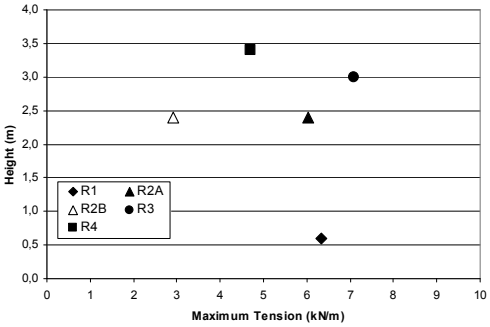

Figure 8. Maximum reinforcement tension vs. depth.

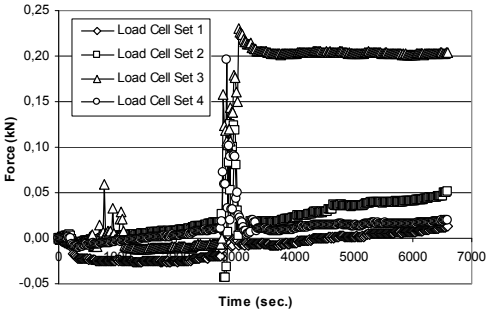

Figure 9. Tension measured in reinforcement R4 – before, during and after compaction operations (Riccio & Ehrlich 2009).

A specific device was designed and used to monitor the vertical and horizontal internal loads on blocks that composed the wall face. Figure 10 shows the measured vertical and horizontal internal loads acting on the instrumented block at different stages of wall construction. Vertical loads were measured at the front (V1) and rear (V2) of the block and horizontal forces (H) in the center. At the end of construction, the measured horizontal force was equal to 41% of the vertical force acting on the block (V1 + V2).

In Figure 10 the dashed line indicates the calculated vertical loads corresponding to the self weight of the blocks full of gravel, assuming the vertical piling of these blocks. Note that the actual facing inclination is not vertical but 1H:10V. The measured values were always higher than those calculated in Figure 10. These results indicate that there was friction mobilization at the soil–block interface and stress transference to the blocks from the backfill.

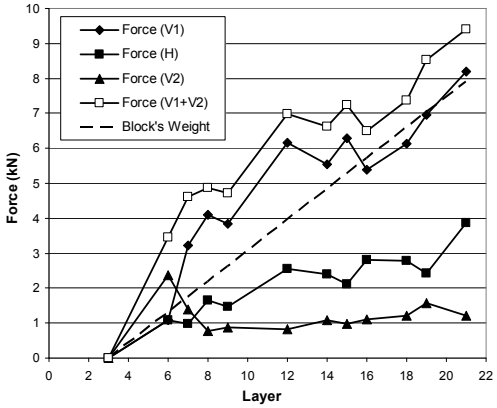

Figure 10. Vertical and horizontal forces on instrumented block (Riccio and Ehrlich 2009).

The relationship between the measured and predicted summation of maximum reinforcement tensions is shown in Figure 11. The methods used in the analysis were those of Bathurst et al. (2003), Ehrlich and Mitchell (1994), Leshchinsky and Boedeker (1989) and Rankine's Theory. The calculations used soil strength parameters determined from plane-strain tests (Table 3) and the measured forces mobilized in the block facing. In order to verify the significance of the results, calculations with and without soil cohesion were carried out.

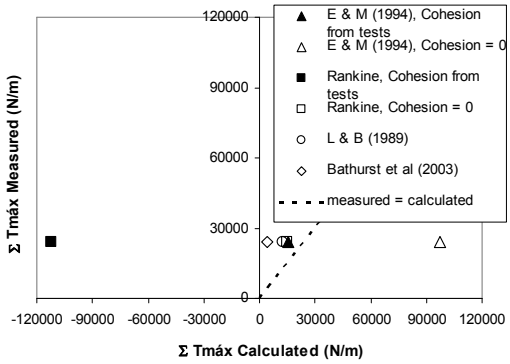

Figure 11. Measured and predicted summation of maximum tension in the reinforcements R1, R2A, R3 and R4 (Riccio and Ehrlich 2009).

Ehrlich and Mitchell (1994) presented the best fit between measurement and prediction. Note that with this method compaction stress, soil cohesion and reinforcement and soil-stiffness properties can be explicitly taken into account. Leshchinsky and Boedeker (1989) presented good results, although possibly due to error compensation. Note that Leshchinsky and Boedeker's (1989) method does not take into account either soil cohesion (which may lead to a reduction in the predicted reinforcement tension) or the stress induced by backfill compaction (which may lead to an increase in predicted reinforcement tension).

For the no cohesion condition Rankine's active and Leshchinsky and Boedeker (1989) give similar reinforcement tension values. Nevertheless, Rankine's active condition leads to negative reinforcement tension values when cohesion is considered.

This means that in this case reinforcement is not necessary for equilibrium. Bathurst et al.'s (2003) method provided a tension value significantly smaller than that measured. The difference in results occurs even though this method does not take into account soil cohesion in the analysis.

The case studies discussed above clearly demonstrate that fine-grained tropical soils are excellent backfill material for reinforced soil wall construction, in spite of their high percentage of fines. The effect of wall facing and soil compaction on the behavior of the structures was also indicated.

4 PHYSICAL MODELING STUDIES

4.1 *Introduction*

Full-scale physical modeling studies of reinforced soil walls were carried out in a facility at COPPE/UFRJ's Geotechnical Laboratory. The effect of soil compaction, reinforcement stiffness, facing type and inclination on the behavior of reinforced soil walls was assessed. Twenty-seven walls have been built to date. Some of the results are presented and discussed here.

4.2 *Model*

In Figure 12 a section of the model is shown. The experiments were performed inside a box composed of a U-shaped concrete wall that is 1.5 m high, 3.0 m long and 2.0 m wide. The lateral faces of the concrete wall received a lubricated polyethylene coating (silicon grease covered by plastic sheets) in order to assure a plane strain condition during the tests. Geogrids were used as reinforcement (Fortrac 80/30-20) and the backfill material was well-graded sand (crushed quartz $C_u = 8.9$).

Vertical loads up to 100 kPa were applied at the top of the backfill using airbags. The constructed model simulates the behavior of a 7.0-m high wall, representing a portion of the prototype (Figure 13).

Two different types of facings were used in the tests: segmental concrete blocks and sacks of sand. The wall face inclination varied from 60° to 85° in the studies in which sacks of sand were used.

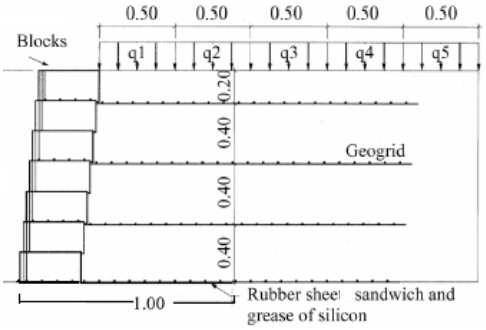

(a)

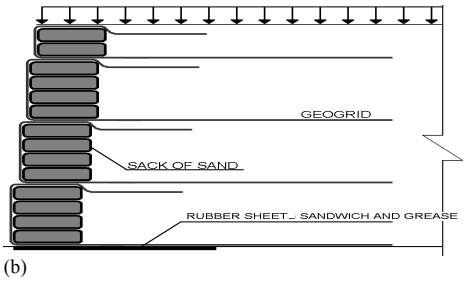

(b)

Figure 12. Model wall section: (a) concrete blocks; (b) sacks of sand.

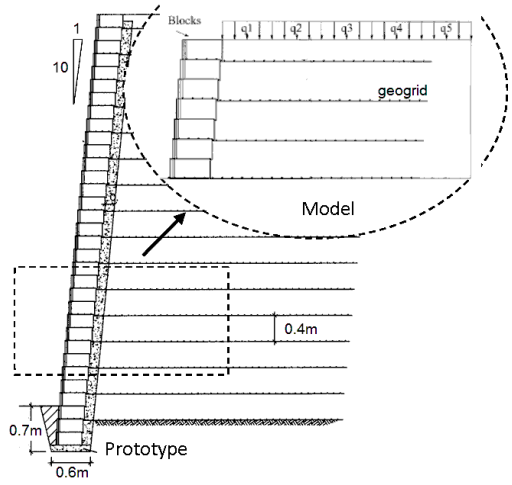

Figure 13. Model vs. prototype.

4.3 *Wall construction*

Four layers of geogrid reinforcements with a 0.4 m vertical spacing and 2.12 m in length were used. For soil compaction two different types of compactors were used: a light vibrating plate (Dynapac LF 81) and a heavy hand driven compactor (Dynapac LC 71-ET). The vertical induced stress due to soil compaction using the light vibrating plate is 8 kPa and that from the heavy hand compactor is 73 kPa. Soil layers 0.2 m thick were put in place dry and then compacted. After compaction using the vibratory tamper the measured soil unit weight was 21 kN/m³. Triaxial tests performed on specimens compacted to this density led to a soil friction angle equal to 42º. Figure 14 shows an illustrative photo of the model wall construction.

The first layer at the base of the wall stands partially on a sandwich of rubber sheets and silicon grease (Figure 12). The objective of this lubricated 1.0-m wide zone was to move the potential failure surface away from the wall face, in order to assure an increase in the dimension of the active zone and facilitate measurements of the tension along the reinforcements.

The reinforcement loads were monitored by groups of load cells installed at four points along each reinforcement layer (see Figure 14). Further details about these load cells can be found in Saramago and Ehrlich (2005). Horizontal displacement of the wall's facing was monitored through four LVDTs. The internal horizontal displacement was monitored by telltales.

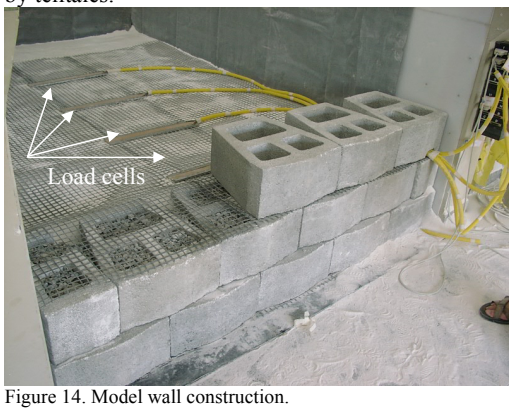

Figure 14. Model wall construction.

4.4 *Results and analysis*

4.4.1 *Effect of soil compaction*

Analyses of results of the modeling studies of reinforced soil walls show that compaction may be a decisive factor in mobilizing tension in the reinforcements and reducing post-construction movements. The results show that compaction is not limited to the reduction in the void ratio. Compaction may also lead to a significant increase in the horizontal stress inside the reinforced soil mass and generate a kind of over-consolidated material.

Figures 15 and 16 show the tension measured along the 4th layer of reinforcement for Wall 1 and Wall 2, respectively (Saramago and Ehrlich 2005). In these figures, curves related to different construc-

tion stages and different steps of external load application are shown. Except for soil compaction, both walls were constructed in the same way, using the same procedure and materials as described above. For Wall 1 a light vibrating plate was used for soil compaction only, while for Wall 2, soil compaction was accomplished using both the vibrating plate and the vibratory tamper.

A clear tendency of the reinforcement tension to be higher next to the face of the wall when the 7th soil layer was placed can be observed in Figures 15 and 16. This tendency remained unaltered after the compaction of the layer with the vibrating plate (for both Walls 1 and 2) and also during the period of external load application (for Wall 1, Figure 15).

Nevertheless, for Wall 2 the mobilized reinforcement tension next to the wall face decreased drastically and was reduced to zero after the compaction of the soil layer with the vibratory tamper (Figure 16). In this wall the reinforcement tension next to the face was always lower after this stage of construction. Note that the compaction of the soil layer with the vibratory tamper led to a significant increase in the maximum tension in the reinforcement, T_{max}. Figure 16 also shows the significant increase in the tensile forces in the reinforcements during the final stages of external load application.

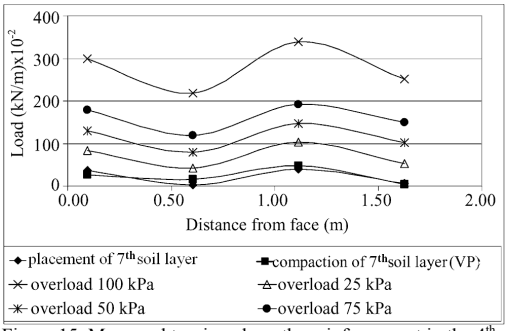

Figure 15. Measured tension along the reinforcement in the 4th reinforcement layer – Wall 1 (Saramago and Ehrlich 2005).

In Figure 17 the dashed and dotted vertical line represents the compaction equivalent influence depth (Z_c) related to the maximum vertical stress induced during soil compaction ($\sigma'_{zc,i}$). The equivalent depth of a soil layer (Z_{eq}) corresponds to the value of the external load applied at the top of the wall divided by the unit weight of the soil (q/γ) plus the real depth of that layer relative to the soil surface. The equivalent vertical stress for the vibratory tamper is equal to 73 kPa. Thus, Z_c for Wall 2 is equal to 3.5 m ($Z_c = \sigma_{zc,i} / \gamma$). It can be observed that T_{max} exhibits a small variation when Z_{eq} is lower than Z_c, i.e., T_{max} is under the influence of compaction. On the other hand, for higher Z_{eq} values there is a linear relationship between T_{max} and Z_{eq}, thus indicating that the compaction effect has vanished and the tension in the reinforcements is controlled only by soil weight.

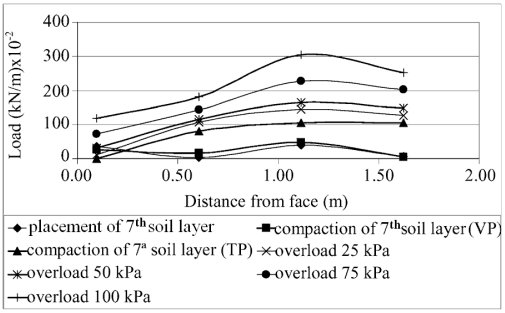

(VP) – Vibrating Plate; (TP) – Tamper Plate

Figure 16. Measured tension along the reinforcement in the 4th reinforcement layer –Wall 2 (Saramago and Ehrlich 2005).

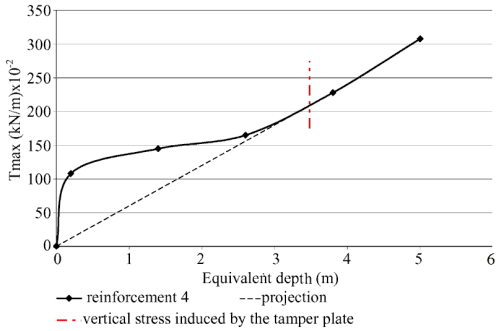

Figure 17. T_{max} vs. equivalent depth for the 4th reinforcement layer – Wall 2 (Saramago and Ehrlich 2005).

Figure 18 shows the measured horizontal displacements in Wall 2 during the application of an external load (q) at the top of the wall through the airbags. In the figure the vertical line represents the vertical stress induced by the vibratory tamper (equal to 73 kPa). Horizontal displacements at the face were measured by the LVDTs in the block facing (LVDTs: A, B, C and B positioned in the 7th, 5th, 3rd, and 1st block layers, respectively). Note that the lateral movements were quite small before the external load, q, reached the value of the vertical induced stress due to soil compaction by the vibratory tamper.

The results shown in Figure 17 and Figure 18 clearly demonstrate that soil compaction can be considered as a kind of soil over-consolidation, in accordance with Ehrlich and Mitchell (1995). Soil compaction pre-stresses the soil and reinforcement and reduces post-construction movements.

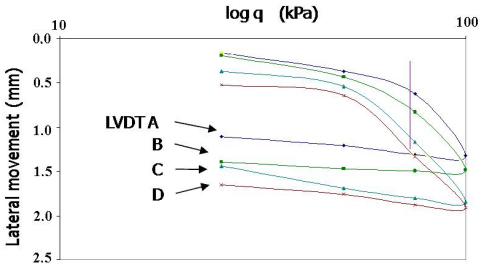

Figure 18. Lateral movements measured by the LVDTs vs. external vertical load, q (Saramago 2002).

4.4.2 *Facing inclination*

Figure 19 presents the summation of measured maximum tension in the reinforcement in walls with a facing of sand sacks and 60º, 75º and 85º inclination during the application of an external load of 100 kPa. It can be seen that the maximum tension increases with facing inclination (Guedes and Ehrlich 2006).

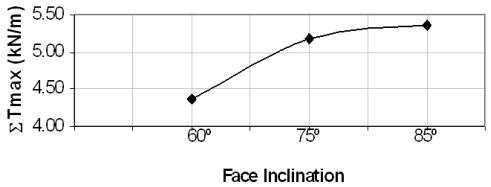

Figure 19. Summation of the measured maximum tension in the reinforcements vs. inclination of the wall face (Guedes and Ehrlich 2006).

4.4.3 *Facing stiffness*

Figure 20 shows the summation of measured maximum tension mobilized in the 2nd, 3rd and 4th reinforcement layers with the equivalent depth, Z_{eq}, for Wall 2 and Wall 3 (85º inclination of wall face), respectively (Guedes and Ehrlich 2006). In this figure curves related to different construction stages and different steps of external load application up to 100 kPa are shown. Wall 3 and Wall 2 were constructed using sacks of sand and block facing, respectively. Except for the facing both walls were constructed in the same way, using the same procedure and material, as described above. Soil compaction was accomplished using both the vibrating plate and the vibratory tamper. Note that for both walls the first layer at the base partially stood upon a sandwich of rubber sheets and silicon grease (see Figure 12).

The facing is not supposed to affect the internal stability. However, Tatsuoka et al. (1989) showed that stiffer faces promote higher confinement of the soil near the face, reducing structure deformations. Tatsuoka (1993) and Tajiri et al. (1996) demonstrated that a rigid face can reduce the tension required along the reinforcements.

Nevertheless, in Figure 20 it can be seen that the facing type does not significantly affect the summation of the maximum tension mobilized in the reinforcement layers. Note that for both walls the mobilized shear stress at the base of the face may be ignored due to lubrication. This demonstrates that the reduction in reinforcement tension due to facing stiffness may be associated with the shear stress mobilization at the base of the wall facing rather than to the facing stiffness itself. This statement could be supported by analyzing the equilibrium forces mobilized in a reinforced soil wall, as represented in Figure 21.

Figure 21 shows the forces in a reinforced soil wall, including the mobilized force at the base of the facing (F_2), where W_s, W_f and F_1 are the weight of the soil wedge, the weight of the facing and the mobilized reaction of the stable soil mass at the potential failure surface, respectively. This simple approach shows that increasing the shear stress mobilization (ϕ_{bf}) at the base of the facing would reduce the summation of maximum tension in the reinforcements (ΣT_{max}).

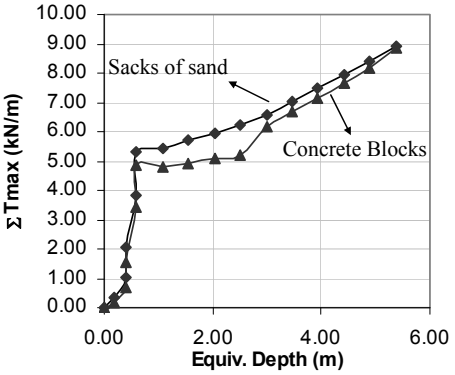

Figure 20. Comparison of measured summation of maximum tensions in the reinforcement layers for walls with different facings.

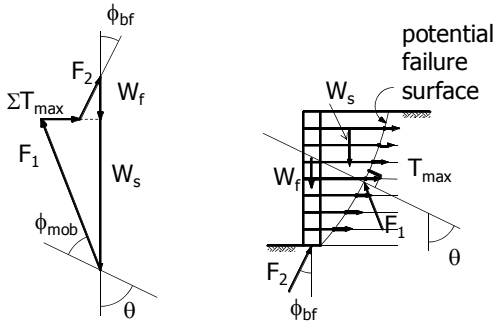

Figure 21. Mobilized forces in a reinforced soil wall.

5 NUMERICAL STUDIES

5.1 *Introduction*

FEM studies of reinforced soil walls and slopes were performed. The mechanism and behavior and the capability of analytical procedures to model the actual behavior were verified.

5.2 *Facing effects*

Parametric FEM studies of a 5-m high reinforced soil wall were performed (Loiola 2001). Figure 22 shows the results of non-dimensional values of summation of the maximum tension in the reinforcements ($\Sigma T_{max}/\gamma H^2$) versus wall face stiffness (EI) for different values of reinforcement stiffness S_i (as defined by Ehrlich and Mitchell 1994). The backfill material was modeled as a cohesionless soil with a 35° friction angle.

Figure 22 shows that the tension in the reinforcements varies with reinforcement stiffness, but that there is no variation in relation to facing stiffness. Nevertheless, for the no facing condition a significant increase in the mobilized tension in the reinforcements occurs, as expected, in accordance with the simple model shown in Figure 21 (W_f and F_2 = 0).

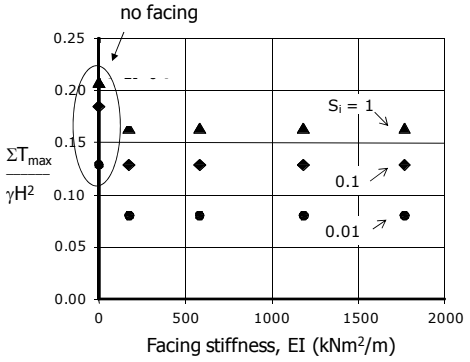

Figure 22. FEM values of summation of the maximum tension in the reinforcements vs. wall face stiffness (Loiola 2001).

5.3 *Numerical and analytical predictions*

Figure 23 compares numerical and analytical predictions (Dantas 2004). A 10-m high reinforced soil wall and cohesionless backfill soil with a 30° friction angle was modeled. Modeling of soil compaction was performed using the procedure shown in Dantas and Ehrlich (1999) and Dantas and Ehrlich (2001). The results determined using the Ehrlich and Mitchell (1994) analytical procedure show a good fit to the FEM results.

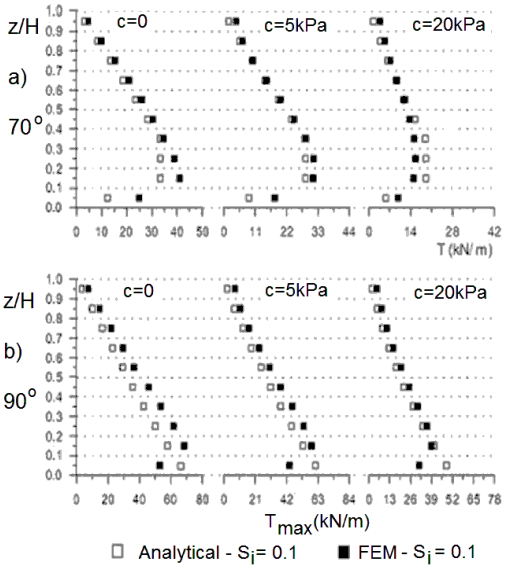

Figure 23. Comparison of numerical and analytical predictions.

6 CONCLUSIONS

Case studies and numerical and physical modeling results were presented and discussed. Measured and calculated values were compared and the prediction capability of available procedures was verified.

Ehrlich and Mitchell (1994) presented the best fit between measurement and prediction. Limit equilibrium and empirical methods have shown a lack of prediction capability. Such methods do not explicitly take into consideration important factors such as soil and reinforcement deformability and the induced stress due to soil compaction.

Monitored reinforced soil structures in Brazil have shown good performance, in spite of the high percentage of fines in the residual tropical soils used as backfill. This behavior is related to the good geotechnical properties of tropical fine-grained soils. Residual soils are an excellent backfill material for reinforced soil structures.

Tropical fine-grained soils, no matter what their percentage of fines, generally show good compaction and workability characteristics. The compacted soil has a high strength, low compressibility and low permeability. Good shear resistance parameters are usually observed.

A 10-meter high geotextile soil slope built using two different types of reinforcement was monitored. In spite of the lower unconfined stiffness of the nonwoven geotextile, movements were systematically lower in the half of the slope in which a nonwoven geotextile was used compared to the other half

in which a stiffer woven geotextile was used. Note that both geotextiles have the same unconfined tension resistance. Analysis of the measurements taken showed that this behavior may be related to the influence of confinement on nonwoven geotextile stiffness.

Analyses of results of case studies and physical and numerical modeling of reinforced soil structures showed that compaction may be a decisive factor in mobilizing tension in the reinforcements and reducing post-construction movements. The results showed that soil compaction is not limited to the reduction in the soil void ratio. Compaction may also lead to a significant increase in the horizontal stress inside the reinforced soil mass and generate a kind of over-consolidated material.

It was also shown that facing may lead a reduction in the tension required in the reinforcements. Numerical and physical modeling demonstrated that this behavior is not associated with facing stiffness itself, but with the shear stress mobilization at the interface of the facing base and foundation soil.

ACKNOWLEDGMENTS

The authors would like to thank HUESKER Synthetics Co., the Brazilian Research Council (CNPq), Rio de Janeiro State Research Funding Agency (FAPERJ) and the José Bonifácio University Foundation (FUJB) for the financial support of these research activities.

REFERENCES

Abramento, M. and Whittle, A. J. 1993. Shear-lag analysis of a planar soil reinforcement in plane strain compression. *Journal of Engineering Mechanics, ASCE*, 119(2), 270–291.

Adib, M. E. 1988. *Internal Lateral Earth Pressure in Earth Walls*. PhD thesis, University of California, Berkeley, Calif.

Andrawes, K. Z., MacGown, A. and Kabir, M. D. H. 1984. Uniaxial strength testing of woven and nonwoven geotextiles. *Geotextiles and Geomembranes*, 1, 41–56.

Bathurst, R. J., Allen, T. and Walters, D. 2003. Reinforcement loads in geosynthetic walls and the case for a new working stress design method, *56CGS/NAGS Conf*., Manitoba, Vol. 1, pp. 56–72.

Becker, L. D. B. 2006. *Behavior of Geogrids in Reinforced Soil Walls and under Pullout Test*. D.Sc. thesis, Pontifical Catholic University of Rio de Janeiro (in Portuguese).

Bishop, A. W. 1955. The use of the slip circle in the stability analysis of earth slopes. *Geotechnique*, 5, 7–17.

Bruno, A. C. and Ehrlich, M., 1997. Performance of a geotextile reinforced soil wall, *2nd Pan-American Symp. on Landslides*, Rio de Janeiro, Vol. 2, pp. 665–670.

Bueno, B. S., Vilar, O. M. and Zornberg, J. G. 2006. Use of tropical soils as backfill of reinforced soil structures in Brazil. *Proceeding of the 8th International Conference on Geosynthetics*, Yokohama, Japan, Vol. 3, 1209–1212.

Carvalho, P. A., Wolle, C. M. and Pedrosa, J. A. B. A. 1986. Reinforced soil embankment using geotextile – An alternative for geotechnic engineering.. *8th Brazilian Conf. of Soil Mech. and Found. Eng.,* Porto Alegre, 168–178 (in Portuguese).

Dantas, B. T. and Ehrlich, M. 1999. Abacus for reinforced soil slopes design under working stress conditions. *1st South American Symposium on Geosynthetics / 3rd Brazilian Symposium on Geosynthetics*, Rio de Janeiro, Vol. 1, 115–122 (in Portuguese).

Dantas, B. T. and Ehrlich, M. 2000. Analysis method for reinforced soil slopes under working stress condition. *Soils & Rocks, Latin-American Geotechnical Journal*. 23(2), 113–133 (in Portuguese).

Dantas, B. T. and Ehrlich, M. 2001. Parametric FE studies on reinforced soil slopes. *Proceedings of the Fifteenth International Conference on Soil Mechanics and Geotechnical Engineering*, Istanbul, Turkey, Vol. 2, pp. 1571–1574.

Dantas, B. T. 2004. *Analysis of Reinforced Soil Embankment under Working Stress Condition*. D.Sc. thesis, COPPE, Federal University of Rio de Janeiro (in Portuguese).

Duncan, J. M., Byrne, P., Wong, K. S. and Mabry, P. 1980. Strength, stress-strain and bulk modulus parameters for finite element analyses of stresses and movements in soil masses. *Geotech. Engrg. Res. Rep. No. UCB/GT/80-O1,* University of California, Berkeley, Calif.

Duncan, J. M. and Seed, R. B. 1986. Compaction-induced earth pressures under Ko-conditions. *J. Geotech. Engrg.,* ASCE, 112(1), 1–22.

Ehrlich, M., Vianna, A. J. D. and Fusaro, F. 1994. Performance behavior of a geotextile reinforced soil wall. *10th Brazilian Conf. of Soil Mech. and Found. Eng*., Foz de Iguaçu, Vol. 3, pp. 819–824 (in Portuguese).

Ehrlich, M. and Mitchell, J. K. 1994. Working stress design method for reinforced soil walls. *Journal of Geot. Eng*., *ASCE,* 120(4), 625–645.

Ehrlich, M. and Mitchell, J. K. 1995. Working stress design method for reinforced soil walls – closure. *Journal of Geot. Eng*., ASCE, 121(11), 820–821.

Ehrlich, M., Delma, V. and Carvalho, P. 1997. *Recent Developments in Soil and Pavement Mechanics*, ed. Balkema, pp. 415–420.

Ehrlich, M. 1999. Analysis of reinforced soil walls and slopes. Keynote lecture *1st South American Symposium on Geosynthetics / 3rd Brazilian Symposium on Geosynthetics*, Rio de Janeiro, Vol. 2, 73–87 (in Portuguese).

Ehrlich, M. and Dantas, B. T. 2000. Discussion on paper Limit Equilibrium as Basis for Design of Geosynthetic. *J. Geoth. Division*, *ASCE*, 126(3), 283–285.

Ehrlich, M. and Becker, L. 2009. *Reinforced Soil Walls and Slopes: Design and Construction*. Ed. Oficina de Textos (in Portuguese).

Guedes, V. P. and Ehrlich, M. 2006. Influence of soil compaction, facing type and inclination on the behavior of geogrid reinforced soil walls. *Proceedings of the 8th International Conference on Geosynthetics*, Yokohama, Japan, Vol. 4 pp. 1413–1416.

Jewell, R. A. 1980. *Some Effects of Reinforcement on Mechanical Behavior of Soils*. Ph.D thesis, University of Cambridge.

Leshchinsky, D. and Boedeker, R. H. 1989. Geosynthetic reinforced structures. *Journal of Geotech. Eng. Division*, *ASCE*, 115(10), 1459–1478.

Loiola, F. L. P. 2001. *Numerical Studies of Significance of Facing on the Behavior of Reinforced Soil Walls*. M.Sc. thesis, COPPE, Federal University of Rio de Janeiro (in Portuguese).

Mori, R. T., Abreu, F. R. and Pan, Y. P. 1979. Properties of some typical compacted saprolites. *6th Pan. Conf. on Soil Mech. and Found. Eng*., Lima, 583–590.

Riccio, M. and Ehrlich, M., 2009. Performance of a block-faced geogrid wall using fine-grained tropical soils. *17th Int. Conference on Soil Mechanics and Geotechnical Engineering*, Alexandria, Vol. 3, 1877–1880.

Riccio, M. and Ehrlich, M., 2010. Prediction of tension in the reinforcement in a full scale block-faced geogrid reinforced soil wall using fine-grained tropical soil as backfill. *Proceedings of the 9th International Conference on Geosynthetics*,

Saramago, R. P. 2002. *Study of the Effect of Soil Compaction on Reinforced Soil Wall Behavior*. D.Sc thesis COPPE, Federal University of Rio de Janeiro.

Saramago, R. P. and Ehrlich, M., 2005. Physical 1:1 scale model studies on geogrid reinforced soil walls. *16th Int. Conf. on Soil Mechanics and Geotechnical Engineering*, Osaka, Vol. 3, 1405–1409.

Steward, J. E. Willianson, R. and Mohney, J. 1977. Earth reinforcement, chapter 5. In: *Guidelines for Use of Fabrics in Construction and Maintenance of Low–volume Roads*. USDA Forest Service, Portland, Oregon.

Tajiri, N., Sasaki, H., Nishimura, J., Ochiai, Y. and Dobashi, K. (1996). Full-scale failure experiments of geotextile-reinforced soil walls with different facings. *Proc. International Symposium on Earth Reinforcement*, Vol. 1, 525–530, Fukuoka, Kyushu, Japan.

Tatsuoka, F., (1993). Roles of facing rigidity in soil reinforcing. *Proceedings of the International Symposium on Earth Reinforcement Practice*, Vol. 2, pp. 831–870, Fukuoka, Kyushu, Japan.

Tatsuoka, F., Tateyama, M. and Murata, O. (1989) .Earth retaining wall with a short geotextile and a rigid facing. In: *Proc. 12th International Conference on Soil Mechanics and Foundation Engineering*, Vol. 2, pp. 1311–1314, Rio de Janeiro, RJ, Brazil.